



Published in final edited form as:

J Orthop Res. 2010 October ; 28(10): 1391–1398. doi:10.1002/jor.21128.

Musculoskeletal deformities secondary to neurotomy of the superior trunk of the brachial plexus in neonatal mice

H. Mike Kim, Leesa M. Galatz, Rosalina Das, Nikunj Patel, and Stavros Thomopoulos
Department of Orthopaedic Surgery, Washington University, St. Louis, Missouri

Abstract

The developmental course of musculoskeletal deformities in neonatal brachial plexus palsy (NBPP) has not been studied extensively. The goals of this study were to: (1) evaluate a new animal model of NBPP, (2) characterize the development of musculoskeletal abnormalities in paralyzed shoulders, and (3) investigate the expression of myogenic and adipogenic genes in paralyzed rotator cuff muscles. Neonatal mice were divided into Neurotomy and Sham groups. The Neurotomy group underwent surgical transection of the superior trunk of the brachial plexus within 24 hours of birth. The Sham group underwent the same surgical exposure, but the brachial plexus was left intact. Musculoskeletal deformities were evaluated with radiological and histological assays at 2, 4, 8, 12, and 30 weeks after birth. The supraspinatus muscles of a separate group of mice were used to examine expression of myogenic and adipogenic genes at 8 weeks. The neurotomized forelimbs developed deformities similar to those seen in human NBPP. The deformities progressed with age. The denervated supraspinatus muscles showed intramuscular fat accumulation and upregulation of both myogenic and adipogenic genes compared to the normal. The current study presents a useful animal model for future research examining musculoskeletal changes secondary to neonatal nerve injury.

Keywords

shoulder deformity; postnatal development; brachial plexus palsy; animal model

INTRODUCTION

Most children affected by neonatal brachial plexus palsy (NBPP) recover spontaneously during the first few months, but approximately 20% of affected children are left with permanent deficits.^{1,2} The permanent deficits commonly described in the literature include internal rotation and adduction contracture of the shoulder, loss of active elbow flexion, osseous deformities (e.g., hypoplasia and dysplasia of the humerus and scapula, posterior subluxation or dislocation of the glenohumeral joint), and muscle atrophy.³⁻⁷ In our previous studies, the developmental course of the musculoskeletal deformities secondary to neonatal shoulder paralysis was investigated with the use of botulinum-toxin-A-induced paralysis in neonatal mice.⁸⁻⁹ Those studies showed that shoulders injected with botulinum toxin develop deformities similar to human NBPP and rotator cuff muscle atrophy and accumulate fat. However, it was not clear whether the deformities and intramuscular fat accumulation seen in the botulinum-toxin-injected shoulders were truly due to the muscle paralysis or due to the effects of the toxin. In order to answer this question, it is necessary to develop an animal model that represents neurogenic paralysis of the shoulder muscles in the

immediate postnatal period. The goals of the current study were to: (1) evaluate a new animal model of NBPP utilizing surgical transection of the brachial plexus, (2) characterize the development of musculoskeletal abnormalities in paralyzed shoulders, and (3) investigate the expression of myogenic and adipogenic genes in paralyzed rotator cuff muscles. We hypothesized that: (1) transection of the brachial plexus in postnatal mice would cause musculoskeletal deformities similar to those seen in human NBPP, (2) the deformities would progress with age, and (3) myogenic genes would be downregulated and adipogenic genes would be upregulated in the paralyzed rotator cuff muscles.

MATERIALS AND METHODS

Animal Model

Fifty one CD-1 neonatal mice were used after approval by the Washington University Animal Studies Committee. There were two surgical groups: Neurotomy and Sham. Mice in the Neurotomy group (n=25) underwent microsurgical transection of the superior trunk of the brachial plexus in the left shoulder within 24 hours of birth. Mice in the Sham group (n=20) underwent the same surgical exposure in the left shoulder, but the brachial plexus was left intact. The right shoulders of the mice of both groups were left intact to serve as normal contralateral controls. The Neurotomy group mice were euthanized at 2, 4, 8, 12, and 30 weeks after the procedure, and the Sham group mice at 2, 4, 8, and 12 weeks with use of CO₂ (n=5 per time point) for radiological and histological assays. A separate group of six mice were allocated for gene expression assessment (3 neurotomized mice and 3 normal mice).

Surgical Techniques

Isoflurane inhalation was used for anesthesia. The neonatal mice were placed on the stage plate of a dissecting microscope in the right lateral decubitus position. A 3-mm skin incision was made in the coronal plane on the left shoulder. After splitting the trapezius, the superior trunk of the brachial plexus and its immediate branch, the suprascapular nerve, were identified and completely transected with micro iris scissors. The wound was closed with 6-0 prolene suture. No postoperative antibiotics or immobilization was used.

Gross Observation

The active motion of the left forelimb was graded once a week following the surgical procedure to evaluate paralysis. Grading was performed based on a scale of 0 to 3. A grade of 0 indicated no paralysis, 1 indicated absent shoulder abduction and flexion with a weak elbow flexion, but well preserved wrist motion, 2 indicated absent shoulder abduction and flexion, absent elbow flexion, and weak wrist extension, and 3 indicated full paralysis of the entire forelimb.

Plain Radiography

Plain radiography was performed as previously described.⁸ Following euthanasia, radiographs were taken with the shoulders fully abducted and the elbow fully extended in the supine position. The radiographs were digitized and analyzed with Image J (National Institutes of Health, Bethesda, Maryland) to measure the maximum glenohumeral abduction angle to assess the adduction contracture of the shoulder (Fig. 1).

Range of Motion Assessment and Micro-computed Tomography (μ CT) Scanning

The range of motion of both elbows of each mouse was measured with a goniometer to evaluate extension contracture of the elbow. Both shoulders were dissected to obtain the entire scapula-rotator cuff-humerus unit. Specimens were then fixed in 4%

paraformaldehyde overnight, dehydrated in graded alcohol, and then scanned with a micro-computed tomography scanner (μ CT 40; Scanco Medical, Basserdorf, Switzerland). Two-dimensional horizontal-plane images of the glenohumeral joint were obtained to assess joint congruity. The specimens were then dissected further to separate the humerus from the scapula. The supraspinatus was kept attached to the humeral head. The supraspinatus-humerus unit and the scapula were separately scanned with μ CT to evaluate various anatomical parameters.

Evaluation of Anatomical Parameters and Histology

Various anatomical parameters were evaluated for the severity of shoulder deformity as previously described⁸: 1) maximum glenohumeral abduction angle with radiographic images using Image J (Fig. 1), 2) maximum elbow flexion angle using a goniometer during dissection, 3) glenohumeral joint congruity on horizontal-plane μ CT images, 4) supraspinatus muscle volume using μ CT, 5) humeral length using μ CT, 6) anteroposterior diameter of the humerus at the distal 1/3 of the diaphysis using μ CT, 7) amount of mineralized bone in the humeral head using μ CT, 8) osseous architecture of the humeral head by measuring the trabecular thickness (Tb. Th), number (Tb. N), and space (Tb. Sp) using μ CT, 9) the areas of the glenoid fossa and scapula with 3D μ CT images, and 10) the version of the humeral head and glenoid with 2D horizontal-plane μ CT images.⁸ It was noted that, unlike humans, the humeral head of mice faces posteriorly rather than medially when the forearm is in neutral rotation. Because of this anatomical difference, version of the humeral head of mice was referred to as “introversion” or “extroversion” instead of “anteversion” or “retroversion”. Following μ CT scanning, each supraspinatus-humerus unit was embedded in paraffin and sectioned (5 μ m thick) in the coronal plane. The sections were stained with either Haematoxylin & Eosin or Toluidine Blue and were evaluated for the morphology of the humeral head and supraspinatus muscle/tendon/entheses.

Gene Expression (Real-time PCR)

A separate group of mice (3 neurotomized mice and 3 normal mice) were euthanized 56 days after birth for mRNA expression analysis. The supraspinatus muscles were dissected, frozen immediately with use of liquid nitrogen, and stored at -80°C for further processing. Total RNA was isolated using the TRIspin method¹⁰. RNA extraction and DNase treatment was performed using the RNeasy mini-kit and DNase I (Qiagen, CA) following manufacturer’s instructions. RNA yield was quantified using a NanoDrop spectrophotometer (Thermo Scientific, DE). Five hundred nanograms of RNA was reverse-transcribed to cDNA using Superscript III RT kit (Invitrogen, CA) following manufacturer’s instructions. Real time PCR reactions were performed using Sybr Green chemistry on a 7300 sequence detection system (Applied Biosystems, CA). The target genes examined were: myogenic transcription factors Myogenin, MyoD1, Myf5 and Myf6, myogenic markers Myh4 (fast myosin heavy chain type IIb isoform) and Myh7 (slow myosin heavy chain type I isoform), adipogenic transcription factors CCAAT/enhancer binding protein alpha (C/EBP α) and Peroxisome Proliferator-Activated Receptor gamma2 (PPAR γ 2), and adipogenic markers Lipoprotein lipase, Leptin, and Glucose Transporter 4 (GLUT4). GAPDH was used as a housekeeping gene. Results were expressed as fold change (Neurotomy/Normal) and were calculated using the Delta Delta Ct method.¹¹

Statistical Methods

Paired t-tests were used for comparisons between the operative shoulders and contralateral normal shoulders within a group at a time point. To evaluate the effect of the duration of paralysis, the ratio of the neurotomized shoulder to the contralateral normal shoulder was calculated for each outcome measure of each mouse. The natural logarithm of each ratio was

used for an analysis of variance (ANOVA) with planned polynomial contrasts. A p value of < 0.05 was considered significant. The data are shown as the mean \pm standard deviation.

RESULTS

Gross Observation

Mice in the Neurotomy group developed an abnormal posture immediately after the procedure (internal rotation, adduction, and extension of the shoulder; full extension of the elbow; mild flexion of the wrist) (Fig. 2). The average paralysis grade was 1.9 ± 0.4 . None of the sham-operated or contralateral normal forelimbs showed a sign of paralysis (average grade = 0 ± 0). At the time of dissection, the neurotomized forelimbs showed severe atrophy of the supraspinatus, infraspinatus, teres minor, subscapularis, deltoid, and biceps brachii while the sham-operated forelimbs did not show any appreciable muscle atrophy.

Joint Ranges of Motion

The maximum glenohumeral abduction and elbow flexion angles were significantly less in the neurotomized shoulders than in the contralateral normal shoulders ($p < 0.05$) (Fig. 3). There was a trend for an increase of angle differences with age between the neurotomized shoulders and contralateral normal shoulders, but this did not reach statistical significance ($p = 0.059$ for glenohumeral angle and $p = 0.076$ for elbow angle). The Sham group did not show any significant differences in either angle between the operated shoulders and the contralateral normal shoulders.

Anatomical Parameters

Supraspinatus muscle volume gradually increased with age in the normal shoulders and was significantly lower throughout all time points in the neurotomized shoulders ($p < 0.05$) (Fig. 4). The Sham group did not show a significant difference between the shoulders except for the 4 week time point. Results for mineralized bone volume and osseous architecture of the humeral head (Tb. Th, Tb. N, and Tb. Sp) demonstrated a significant delay in mineral accumulation in the humeral head of the neurotomized shoulders (Fig. 4, Table 1). The Sham group did not show any significant differences between the shoulders except for humeral bone volume at 2 weeks. The humeral head of the neurotomized shoulders showed flattening at the posterior aspect (Fig. 5). The humeral length was significantly decreased in the neurotomized shoulders ($p < 0.05$) at all time points except 12 and 30 weeks. The anatomical parameters of the scapula (i.e., areas of the entire scapula and glenoid fossa) showed a significant delay of scapular growth in the neurotomized shoulders. The Sham group did not show any significant differences between the shoulders. There was an overall trend for increasing differences between the neurotomized and contralateral normal shoulders with age in these anatomical parameters. Among these, supraspinatus muscle volume, Tb.Th., humeral diaphysis diameter, and scapular area showed a statistically significant trend ($p < 0.01$).

The mean humeral head version was significantly increased in the neurotomized shoulders compared to the contralateral normal shoulders at 8 and 12 weeks ($p = 0.004$ and 0.02 , respectively), indicating increased humeral introversion in the neurotomized shoulders (Fig. 6). At 30 weeks, there was no identifiable humeral head articular surface, and thus, it was impossible to measure the humeral head version. The mean glenoid version was significantly decreased in the neurotomized shoulders at all time points ($p < 0.05$) except for 30 weeks, indicating increased glenoid retroversion in the neurotomized shoulders (Fig. 6). The Sham group showed no significant differences between the shoulders. Both humeral and glenoid version showed a significant trend for increasing difference between shoulders with age ($p < 0.05$). The congruity of the glenohumeral joint was relatively well preserved until

12 weeks in the Neurotomy group despite the apparent humeral head and glenoid deformities. At 30 weeks, however, the humeral head was found to be subluxated anteriorly, and the glenoid showed erosion at the anteroinferior aspect (Fig. 7). The Sham group showed no joint incongruity.

Histology

The humeral head of the neurotomized shoulders showed loss of the normal sphericity with abnormally thin articular cartilage (Fig. 8). The supraspinatus insertion on the humeral head of the neurotomized shoulders showed delayed maturation of the transitional fibrocartilaginous structure throughout the time points. There was significant fat accumulation in the supraspinatus muscle of the neurotomized shoulders (Fig. 9). At 2 weeks, the supraspinatus muscles showed atrophy without fat accumulation. At 4 weeks, fat started to appear within the muscle, and the amount of intramuscular fat increased with age. At 12 and 30 weeks, most of the muscle was replaced by fat, and the total volume of this muscle was substantially decreased.

Real time PCR of the supraspinatus muscle

Myogenin was upregulated by 280 fold in the neurotomized shoulders compared to the normal shoulders (Table 2). MyoD1, Myf5, and Myf6 were also upregulated in the neurotomized shoulders. Expression of the myosin heavy chain fast-twitch type IIb isoform - Myh4 was downregulated while the slow-twitch type I isoform - Myh7 was upregulated. Adipogenic genes C/EBP α , PPAR γ 2, Leptin, and Lipoprotein lipase were all upregulated in the neurotomized shoulders (Table 2). GLUT4 expression was not different between the neurotomized and the normal shoulders.

DISCUSSION

The data from the current study demonstrates that transection of the superior trunk of the brachial plexus in neonatal mice reproduces many important pathological conditions of human NBPP. Paralysis of the forelimb was induced within 24 hours of birth by microsurgical nerve transection, reproducing the immediate postnatal paralysis seen in human infants with NBPP. The neurotomized forelimbs developed a loss of active external rotation, flexion, and abduction of the shoulder, active flexion of the elbow, and active extension of the wrist and digits, which led to adduction and internal rotation contracture of the shoulder and extension contracture of the elbow. There were abnormalities of the humeral head such as hypoplasia, delayed mineralization, and flattening of the posterosuperior aspect. Humeral version was altered (i.e., increased introversion) in the neurotomized forelimbs. There were also abnormalities of the scapula such as hypoplasia and increased retroversion of the glenoid. There was profound atrophy of the supraspinatus, infraspinatus, subscapularis, teres minor, deltoid, and biceps brachii muscles in the neurotomized shoulders. The transection of the brachial plexus in this study resulted in a lower motor neuron lesion causing flaccid paralysis of the affected muscles. Bone and joint deformities are typically seen in lower motor neuron lesions (e.g., due to poliomyelitis, myelomeningocele, or brachial plexus injury) that occur early in the postnatal developmental of musculoskeletal tissues.

The glenohumeral joint developed anterior subluxation or dislocation with erosion of the anteroinferior glenoid. The direction of humeral head subluxation is different from that of human NBPP, in which the humeral head is subluxated posteriorly. The location of glenoid erosion is also different from human NBPP, which has erosion of the posteroinferior glenoid. This difference may be attributed to the different anatomy of the humerus and scapula between mice and humans as previously described. The articular surface of the

human humeral head faces medially when the forearm is in the neutral position, whereas the mouse humeral head faces posteriorly. The mouse scapula is oriented more sagittally than humans, perhaps resulting in different shoulder kinematics.

Our data demonstrates that shoulder deformity secondary to NBPP progresses with age, which is consistent with the findings of clinical studies.^{6,7} The increase in severity of deformity was particularly evident in bony and muscle outcomes. The soft tissue contracture also showed the same trend, but this did not reach statistical significance, which may be due to the small sample size of the study or may indicate a plateau in soft tissue contracture at a certain point. Interestingly, glenoid version showed an opposite trend; the difference between the shoulders decreased with age, and the glenoid was found to be anteverted rather than retroverted at 30 weeks, leading to anterior subluxation of the humeral head. This finding is different from clinical studies, which showed the increase of retroversion of the glenoid with age in children with NBPP.^{4,6,7} This difference may again be attributed to differences in kinematics between mouse and human shoulders.

Denervation of neonatal rotator cuff muscles caused intramuscular fat accumulation and muscle atrophy. The supraspinatus muscle of the neurotomized shoulders showed substantial atrophy at 2 weeks and started to show fat accumulation at 4 weeks. Although it was not quantified, the relative amount of fat appeared to increase with age compared to the muscle. At 30 weeks, the muscle was found to be almost entirely replaced by fat. This finding is consistent with the study of Pöyhiä et al⁵ that showed atrophy and fatty deposition of the rotator cuff muscles in children with NBPP. This microscopic observation was supported by our gene expression studies. Adipogenic genes were upregulated in the neurotomized shoulders compared to normal. Interestingly, myogenic genes were also all upregulated in the neurotomized shoulders. Our previous study⁹ showed similar intramuscular fat accumulation in addition to muscle atrophy in botulinum-toxin-injected supraspinatus muscles. This finding is similar to the study of Frey et al¹³ that showed upregulation of both adipogenic and myogenic genes in tenotomized infraspinatus muscles of adult sheep. It is not clear why adipogenic and myogenic genes were both upregulated in denervated neonatal muscles. This may represent an abortive regenerative process of the denervated muscle and resultant loss of the negative feedback inhibition by end products of the process, which leads to the constant upregulation of myogenic genes.

Only a few studies describe the use of animal models for NBPP. Our previous study⁸ used botulinum toxin A to paralyze the shoulders of neonatal mice and reported similar deformities as seen in the current study. The duration of paralysis was varied by controlling the dose of botulinum toxin A, which demonstrated the recovery potential of neonatal shoulders after the return of muscle function. The study of Li et al¹⁴ utilized C5, 6 root neurotomy in rats and reported similar shoulder deformity to the current study. However, they performed the neurotomy at 5 days after birth allowing a substantial delay before the onset of paralysis. They measured glenoid version in histological sections, which likely was not as accurate as the μ CT methods used in the current study.

Our study had several limitations. First, differences in shoulder kinematics of mice compared to humans resulted in humeral version change and humeral head subluxation in directions that were different than those seen in humans. Second, the mice in the Neurotomy group could not bear weight with their neurotomized forelimb because of the paralysis while those in the Sham group used their operated forelimb for weight bearing. It is possible that non-weight bearing may have contributed to the deformity development in the neurotomized shoulders in addition to muscle paralysis. Third, we performed a nerve transection in this study resulting in an irreversible plexus injury. Human NBPP, in contrast, is typically a reversible traction-type injury. A traction injury model would reproduce the pathology of

human NBPP more accurately and will to be examined in future studies. The strengths of the present study include the creation of shoulder paralysis immediately after birth, quantitative and rigorous outcome measurements with validated methods, and the use of real-time PCR to provide adjuvant data for the histological observation of intramuscular fat accumulation.

In conclusion, we report an animal model utilizing surgical transection of the superior trunk of the brachial plexus of mice in the immediate postnatal period to reproduce many important musculoskeletal deformities of human neonatal brachial plexus palsy. As in the human condition, the deformities progressed with age. Intramuscular fat accumulation was found in addition to muscle atrophy in the denervated rotator cuff muscles. The adipogenic and myogenic genes were both upregulated in these muscles. This study presents a useful animal model that may provide a better understanding of musculoskeletal changes secondary to an early postnatal nerve injury and lead to better management of the condition.

Acknowledgments

“This study was funded in part by the National Institutes of Health (AR055580)”.

REFERENCES

1. Adler JB, Patterson RL Jr. Erb's palsy. Long-term results of treatment in eighty-eight cases. *J Bone Joint Surg Am.* 1967; 49:1052–1064. [PubMed: 6038856]
2. Waters PM. Comparison of the natural history, the outcome of microsurgical repair, and the outcome of operative reconstruction in brachial plexus birth palsy. *J Bone Joint Surg Am.* 1999; 81:649–659. [PubMed: 10360693]
3. Hoeksma AF, Ter Steeg AM, Dijkstra P, Nelissen RG, Beelen A, de Jong BA. Shoulder contracture and osseous deformity in obstetrical brachial plexus injuries. *J Bone Joint Surg Am.* 2003; 85-A: 316–322. [PubMed: 12571311]
4. Kambhampati SB, Birch R, Cobiella C, Chen L. Posterior subluxation and dislocation of the shoulder in obstetric brachial plexus palsy. *J Bone Joint Surg Br.* 2006; 88:213–219. [PubMed: 16434527]
5. Poyhia TH, Nietosvaara YA, Remes VM, Kirjavainen MO, Peltonen JI, Lamminen AE. MRI of rotator cuff muscle atrophy in relation to glenohumeral joint incongruence in brachial plexus birth injury. *Pediatr Radiol.* 2005; 35:402–409. [PubMed: 15635469]
6. van der Sluijs JA, van Ouwkerk WJ, de Gast A, Wuisman PI, Nollet F, Manoliu RA. Deformities of the shoulder in infants younger than 12 months with an obstetric lesion of the brachial plexus. *J Bone Joint Surg Br.* 2001; 83:551–555. [PubMed: 11380130]
7. Waters PM, Smith GR, Jaramillo D. Glenohumeral deformity secondary to brachial plexus birth palsy. *J Bone Joint Surg Am.* 1998; 80:668–677. [PubMed: 9611027]
8. Kim HM, Galatz LM, Patel N, Das R, Thomopoulos S. Recovery potential after postnatal shoulder paralysis. An animal model of neonatal brachial plexus palsy. *J Bone Joint Surg Am.* 2009; 91:879–891. [PubMed: 19339573]
9. Thomopoulos S, Kim HM, Rothermich SY, Biederstadt C, Das R, Galatz LM. Decreased muscle loading delays maturation of the tendon enthesis during postnatal development. *J Orthop Res.* 2007; 25:1154–1163. [PubMed: 17506506]
10. Reno C, Marchuk L, Sciore P, Frank CB, Hart DA. Rapid isolation of total RNA from small samples of hypocellular, dense connective tissues. *Biotechniques.* 1997; 22:1082–1086. [PubMed: 9187757]
11. Schmittgen TD, Livak KJ. Analyzing real-time PCR data by the comparative C(T) method. *Nat Protoc.* 2008; 3:1101–1108. [PubMed: 18546601]
12. Moukoko D, Ezaki M, Wilkes D, Carter P. Posterior shoulder dislocation in infants with neonatal brachial plexus palsy. *J Bone Joint Surg Am.* 2004; 86-A:787–793. [PubMed: 15069145]

13. Frey E, Regenfelder F, Sussmann P, Zumstein M, Gerber C, Born W, Fuchs B. Adipogenic and myogenic gene expression in rotator cuff muscle of the sheep after tendon tear. *J Orthop Res.* 2009; 27:504–509. [PubMed: 18932240]
14. Li Z, Ma J, Apel P, Carlson CS, Smith TL, Koman LA. Brachial plexus birth palsy-associated shoulder deformity: a rat model study. *J Hand Surg [Am].* 2008; 33:308–312.

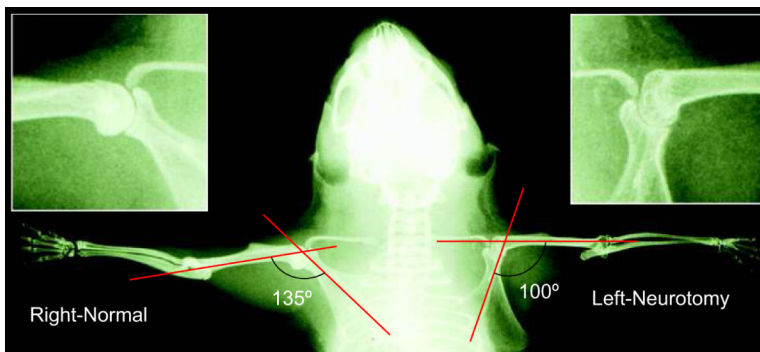


Figure 1. The maximum glenohumeral abduction angle was determined at the intersection of two lines: one along the scapular spine and a second along the long axis of the humerus. Shoulder adduction contracture and humeral head flattening occurred consistently in the neurotomized shoulders compared with the contralateral normal shoulders.

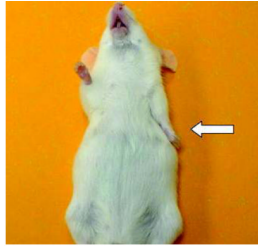


Figure 2. Abnormal posture of the neurotomized forelimb (shoulder extension, internal rotation, and adduction, elbow extension, and mild wrist flexion) observed in a 12-week old mouse.

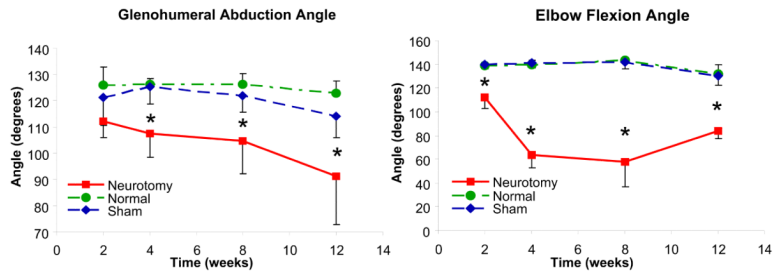


Figure 3.

Glenohumeral abduction and elbow flexion angles were significantly decreased in the neurotomized shoulders. *Significant difference ($p < 0.05$) between the neurotomized and the normal contralateral shoulders. For 30-week old mice: glenohumeral angle = $103.2 \pm 8.3^\circ$ and $126.6 \pm 7.6^\circ$ for the neurotomized and the normal shoulders, respectively ($p = 0.01$); elbow angle = $78 \pm 21^\circ$ and $142 \pm 4.5^\circ$ ($p = 0.002$).

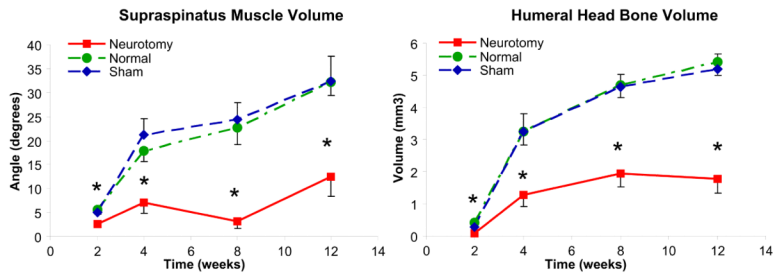


Figure 4. Supraspinatus muscle volume and humeral head mineralized bone volume showed significant decreases in the neurotomized shoulders at all time points. *Significant difference ($p < 0.05$) between the neurotomized and the normal contralateral shoulders. For 30-week old mice: supraspinatus volume = $2.1 \pm 1.1\text{mm}^3$ and $24.1 \pm 8.5\text{mm}^3$ for the neurotomized and the normal shoulders, respectively ($p = 0.005$); humeral head bone volume = $2.2 \pm 0.3\text{mm}^3$ and $4.4 \pm 0.3\text{mm}^3$ ($p = 0.002$).

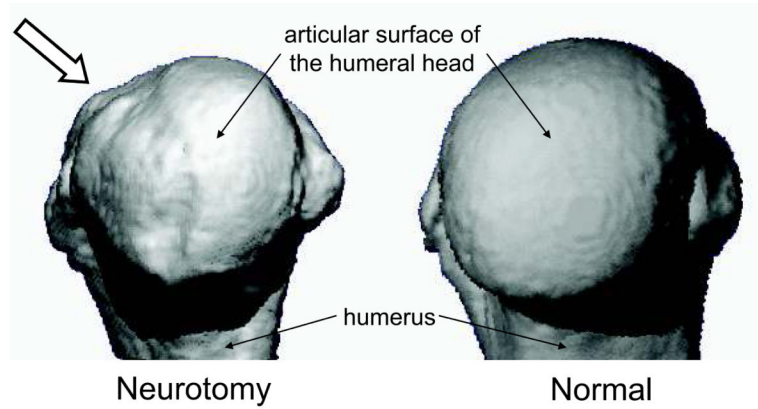
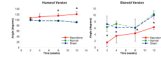


Figure 5. The humeral head of the neurotomized shoulders (left) was small and showed flattening at the posterior aspect (white arrow), whereas the normal shoulders (right) showed a spherical humeral head.

**Figure 6.**

Humeral head version was significantly increased in the neurotomized shoulders at 8 and 12 weeks, and glenoid version was significantly decreased at all time points except 30 weeks, indicating the increased glenoid retroversion in the neurotomized shoulders. For 30-week old mice: glenoid version = $19.4 \pm 12.5^\circ$ and $10.1 \pm 5.5^\circ$ for the neurotomized and the normal shoulders, respectively ($p = 0.29$).

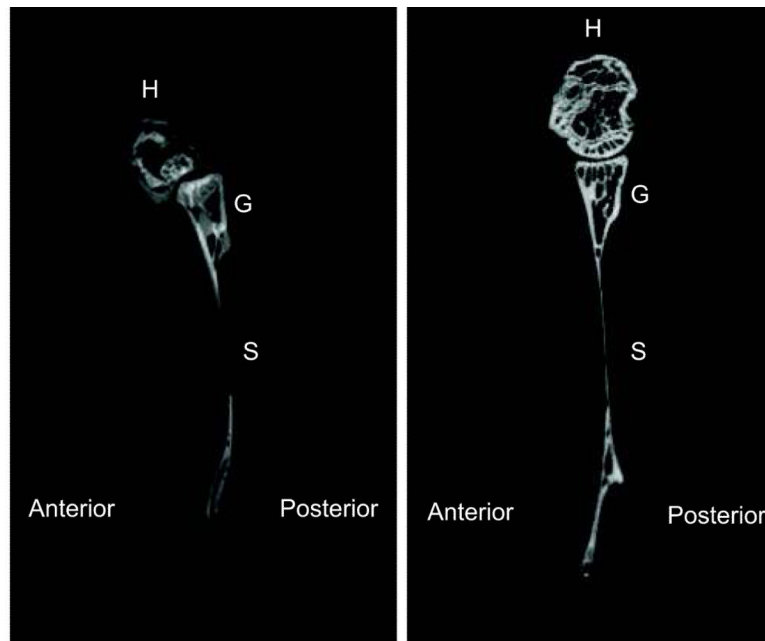


Figure 7. The humeral head was subluxated anteriorly with erosion of the anteroinferior glenoid at the neurotomized shoulder (left) of a 30-week old mouse. The contralateral normal shoulder (right) showed a congruent glenohumeral joint. H = humeral head; S = scapula; G = glenoid.

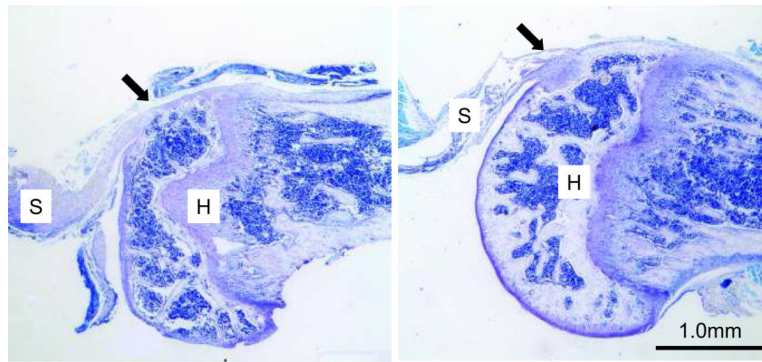


Figure 8.

The neurotomized shoulder (left) of a 12-week old mouse showed substantial deformity of the humeral head such as flattening of posterosuperior aspect of the articular surface and delayed development of the supraspinatus tendon insertion (black arrow), whereas the contralateral normal shoulder shows a round humeral head with a well developed supraspinatus insertion (black arrow). H = humeral head; S = supraspinatus musculotendinous unit (Toluidine Blue stain).

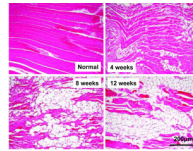


Figure 9. The supraspinatus muscles of the neurotomized shoulders showed progressive fat accumulation in addition to atrophy with age (Haematoxylin & Eosin stain).

TABLE 1

Age [†]	Trabecular thickness (mm)	Trabecular number (number/mm)	Trabecular space (mm)	Humeral length (mm)	Humeral diameter (mm)	Glenoid area (mm ²)	Scapular area (mm ²)
2 weeks							
Neurotomy	0.08 ± 0.01	1.12 ± 0.06	0.91 ± 0.06	7.43 ± 0.25*	0.78 ± 0.05	0.75 ± 0.08*	7.96 ± 0.44
Normal	0.09 ± 0.01	1.02 ± 0.12	1.01 ± 0.13	7.8 ± 0.16	0.78 ± 0.02	0.9 ± 0.06	8.16 ± 0.49
Sham	0.10 ± 0.01	1.48 ± 0.32	0.73 ± 0.16	8.26 ± 0.29	0.8 ± 0.1	0.98 ± 0.12	11.4 ± 2.0
4 weeks							
Neurotomy	0.14 ± 0.03*	2.88 ± 0.52	0.35 ± 0.07	10.8 ± 0.4*	0.86 ± 0.08	1.12 ± 0.03*	21.0 ± 1.7
Normal	0.18 ± 0.02	2.99 ± 0.38	0.39 ± 0.18	11.3 ± 0.3	0.9 ± 0.07	1.38 ± 0.06	22.5 ± 2.1
Sham	0.17 ± 0.01	3.52 ± 0.3	0.3 ± 0.03	11 ± 0.1	0.84 ± 0.05	1.27 ± 0.08	21.4 ± 0.9
8 weeks							
Neurotomy	0.14 ± 0.01*	3.63 ± 1.19	0.32 ± 0.22	11.9 ± 0.7*	0.86 ± 0.13	1.23 ± 0.11*	21.0 ± 2.4*
Normal	0.26 ± 0.02	4.7 ± 0.62	0.16 ± 0.02	12.9 ± 0.2	1.0 ± 0.08	1.6 ± 0.18	31.3 ± 2.5
Sham	0.24 ± 0.02	4.0 ± 0.69	0.17 ± 0.02	12 ± 0.3	0.9 ± 0.07	1.42 ± 0.08	28.0 ± 1.4
12 weeks							
Neurotomy	0.12 ± 0.01*	3.37 ± 0.59*	0.32 ± 0.06*	12.4 ± 0.7	0.89 ± 0.03	1.25 ± 0.06*	31.1 ± 2.7*
Normal	0.21 ± 0.03	4.7 ± 0.62	0.19 ± 0.01	12.8 ± 0.3	0.93 ± 0.08	1.85 ± 0.18	38.4 ± 3.2
Sham	0.24 ± 0.01	5.23 ± 0.2	0.16 ± 0.1	13 ± 0.2	1.0 ± 0.05	1.59 ± 0.05	37.8 ± 1.3
30 weeks							
Neurotomy	0.17 ± 0.03*	3.03 ± 0.79	0.39 ± 0.18	12.7 ± 0.4	0.95 ± 0.06	1.65 ± 0.38	31.3 ± 2.2*
Normal	0.20 ± 0.02	4.03 ± 0.66	0.27 ± 0.1	12.9 ± 0.7	1.28 ± 0.06	1.81 ± 0.09	39.9 ± 2.8
Sham	n/a	n/a	n/a	n/a	n/a	n/a	n/a

The data are shown as mean ± standard deviation.

* Significant differences (p < .05, paired t-test) between the neurotomized and the contralateral normal shoulders in the Neurotomy group.

[†] Neurotomy refers to the neurotomized shoulders of the Neurotomy group; Normal, the contralateral normal shoulders of the Neurotomy group; and Sham, the sham-operated shoulders of the Sham group.

TABLE 2

Classification	Genes	Fold change [*]	p-value [†]
Myogenic	Myogenin	280 ± 137.3	0.002
	MyoD1	19.4 ± 9.4	0.012
	Myf5	10.8 ± 6.7	0.022
	Myf6	4.4 ± 2.5	0.067
	Myh4 (fast twitch)	0.11 ± 0.07	0.020
	Myh7 (slow twitch)	14.7 ± 3.6	0.003
Adipogenic	C/EBP α	37.3 ± 20.2	0.022
	PPAR γ 2	16.2 ± 9.9	0.013
	Leptin	58.3 ± 26.9	0.006
	Lipoprotein Lipase	2.8 ± 0.4	0.006
	GLUT4	1.1 ± 0.2	0.673

* Fold change represents the ratio of the neurotomized shoulders to the normal shoulders.

[†] P-values from one-sample t-test with use of natural logarithms of the ratios